1   **Assessing bulk carbonates as archives for seawater Li isotope ratios**

2

3   Philip A.E. Pogge von Strandmann[1*], Daniela N. Schmidt[2], Noah J Planavsky[3],

4   Guangyi Wei[3], Chloe L. Todd[2]; Karl-Heinz Baumann[4]

5

6   [1]London Geochemistry and Isotope Centre (LOGIC), Institute of Earth and Planetary

7   Sciences, University College London and Birkbeck, University of London, Gower

8   Place, London, WC1E 6BT, UK.

9   [2]School of Earth Sciences, University of Bristol, Wills Memorial Building, Queens

10   Road, Bristol, BS8 1RK, UK.

11   [3]Department of Geology and Geophysics, Yale University, New Haven, CT, 06511,

12   USA.

13   [4]Department of Geosciences, University of Bremen, GEO Building, Klagenfurter

14   Strasse, 28359 Bremen, Germany.

15   *Corresponding author: p.strandmann@ucl.ac.uk

16

17

18   Abstract

19   Silicate weathering is a primary control on the carbon cycle and therefore long-term

20   climate. Tracing silicate weathering in the geological record has been a challenge for

21   decades, with a number of proxies proposed and their limits determined. Recently

22   lithium isotopes in marine carbonates have emerged as a potential tracer. Bulk

23   carbonates are increasingly being used as a Li isotope archive, though with limited tests

24   thus far of the robustness of this approach in the modern ocean. As the bulk composition

25   of marine pelagic carbonates has changed through time and geographically, assessing

26   the fidelity of bulk carbonate as proxy carrier is fundamental. To address the impact of

27   compositional variability in bulk carbonate on Li isotopes, we examine 27 Bahamian

28   aragonitic bulk carbonates and 16 Atlantic largely calcitic core-top sediment samples.

29   Two core-tops only have trace (<10%) carbonate, and are analysed to test whether

30   carbonates in such sections are still a viable archive. We selectively extract the

31   exchangeable and carbonate fractions from the core-top samples. The exchangeable

32   fraction contains ~2% of the total Li and has a fairly constant offset from seawater of

33    $16.5 \pm 0.8‰$. When leaching silicate-containing carbonates, acetic acid buffered with

34   sodium acetate appears a more robust method of solely attacking carbonates compared

35   to dilute HCl, which may also liberate some silicate-bound Li. Carbonates from samples

36   that do not contain aragonite have the isotopic fractionation of seawater of $\Delta^7Li_{seawater\text{-}calcite} = 6.1 \pm 1.3‰$ (2sd), which is not affected by latitude or the water depth the sample

38   was deposited at. The pure aragonite bulk carbonates from the Bahamas have a

39   fractionation of $\Delta^7Li_{seawater\text{-}aragonite} = 9.6 \pm 0.6‰$. A sediment sample from the Galician

40   coast that mostly consists of quartz is highly offset from seawater by ~20‰ and also

41   has relatively high Li/Ca ratios. These high values are not due to leaching of silicate

42   material directly (Al/Ca ratios are low). We interpret this addition via cation exchange

43   of Li from silicate during recrystallisation. Overall bulk carbonates from the open ocean

44   are a reliable archive of seawater δ^7Li, but care must be taken with carbonate

45   mineralogy and low-carbonate samples. Overall, therefore, any examination of the

46   palaeo-seawater δ^7Li record must be reproduced in different global settings (e.g.

47   multiple global cores) before it can be considered robust.

48

49

50

51

1.0 Introduction

Continental silicate weathering is considered to be a fundamental control on the long-term carbon cycle and climate (Chamberlin, 1899; Walker et al., 1981) as weathering provides nutrients for organic carbon formation in the oceans, clay particles to help that organic carbon sink (Hawley et al., 2017), and alkalinity and cations such as Ca and Mg for formation of oceanic carbonate (Berner, 2003). As such, considerable effort has gone into developing methods to reconstruct palaeo-weathering behaviour, to determine the effect it may have on the Earth's short- and long-term climate. Several tracers have been used, but most suffer from not unambiguously being able to distinguish between carbonate and silicate weathering (where only silicate weathering sequesters CO_2), and/or being fractionated by biology (e.g. $^{87}Sr/^{86}Sr$ (Oliver et al., 2003) or stable Ca, Mg or Si isotopes (Fantle and Tipper, 2014; Opfergelt et al., 2010; Pogge von Strandmann et al., 2014)).

One tracer that is gaining increasing interest, as it is unaffected by these processes, is lithium isotopes. Firstly, lithium is concentrated by several orders of magnitude in silicates over carbonates. Consequently, carbonate weathering, even in carbonate-dominated catchments, exerts no influence on riverine Li (Dellinger et al., 2015; Kisakürek et al., 2005; Millot et al., 2010; Pogge von Strandmann et al., 2017b). Secondly, Li isotopes are not fractionated during uptake into plants or phytoplankton (diatoms, cyanobacteria and green algae) (Lemarchand et al., 2010; Pogge von Strandmann et al., 2016).

Riverine δ^7Li values range between 2–44‰, with a global mean of 23‰ (Dellinger et al., 2015; Huh et al., 2001; Huh et al., 1998; Kisakürek et al., 2005; Pistiner and Henderson, 2003; Pogge von Strandmann et al., 2010; Pogge von Strandmann et

76 al., 2006; Pogge von Strandmann et al., 2017b), compared to primary silicate rock δ^7Li

77 values for the continental crust of 0‰ (Sauzéat et al., 2015), and of 3–5‰ for basalt

78 (Elliott et al., 2006). Primary rock dissolution does not cause isotope fractionation, but

79 secondary minerals preferentially take up ^6Li, driving residual waters isotopically

80 heavier (Pistiner and Henderson, 2003; Vigier et al., 2008; Wimpenny et al., 2015;

81 Wimpenny et al., 2010).

82   Therefore, in surface waters, Li isotopes provide information on the ratio of

83 primary mineral dissolution (low δ^7Li), relative to secondary mineral formation

84 (driving δ^7Li high). This ratio is known as the weathering congruency, where congruent

85 weathering involves complete dissolution of the primary rock, and incongruent

86 weathering involves secondary mineral formation (Misra and Froelich, 2012; Pogge

87 von Strandmann and Henderson, 2015). Weathering congruency may be a tracer for the

88 weathering intensity, defined as the ratio of the weathering rate to denudation rate

89 (Dellinger et al., 2017; Dellinger et al., 2015; Pogge von Strandmann et al., 2017b).

90   In the modern oceans, riverine Li makes up approximately 50% of the Li input,

91 with the other half derived from hydrothermal fluids (Chan and Edmond, 1988; Chan

92 et al., 1994; Hathorne and James, 2006). Removal of Li from seawater comes from

93 uptake of Li into altered oceanic crust and authigenic clays, which cumulatively impose

94 a fractionation of around 15‰, driving modern seawater to 31‰. It follows that

95 changes in the riverine Li flux and/or isotope composition due to global weathering

96 changes would leave a fingerprint in the oceans.

97   A number of studies have used Li isotopes in different types of marine

98 carbonates to reconstruct palaeo-weathering conditions (Hall et al., 2005; Hathorne and

99 James, 2006; Lechler et al., 2015; Misra and Froelich, 2012; Pogge von Strandmann et

100 al., 2017a; Pogge von Strandmann et al., 2013; Ullmann et al., 2013). Some of these

101 studies used foraminifera as an archive, but they exhibit species-specific vital effects

102 on Li isotope fractionation, potentially controlled by pH, DIC or temperature (Hall et

103 al., 2005; Hathorne and James, 2006; Misra and Froelich, 2009; Roberts et al., 2018;

104 Vigier et al., 2015). The Cenozoic record of Misra and Froelich (2012) also exhibits

105 significant scatter of >3‰ at single points in time, with error widths of over 6‰.

106 Therefore, increasingly, bulk carbonates are being used to reduce the time of sample

107 processing, and the amount of initial material required. Using bulk material was thought

108 to be viable, because all biogenic and inorganic calcites were thought to impose similar

109 fractionation factors on Li isotopes, of 0–5‰ (Marriott et al., 2004a; Marriott et al.,

110 2004b; Misra and Froelich, 2009; Pogge von Strandmann et al., 2013; Rollion-Bard et

111 al., 2009). Equally, inorganic and biogenic aragonites also exhibit similar fractionation

112 factors of ~11‰ (Dellinger et al., 2018; Marriott et al., 2004a; Marriott et al., 2004b).

113 However, a recent study of biogenic carbonates has exhibited greater, species-specific,

114 variability (Dellinger et al., 2018). Especially modern calcitic molluscs (scallops,

115 clams, mussels and oysters) exhibit δ^7Li values both higher and lower than modern

116 seawater ($\Delta^7Li_{seawater-carb}$ = -10 to +9‰), although brachiopods show a narrow range of

117 fractionation ($\Delta^7Li_{seawater-carb}$ = 3.5–5.5‰) that is similar to inorganic fractionation

118 (Dellinger et al., 2018). Evolutionary changes in the composition from a

119 coccolithophore dominated carbonate in the Paleogene to a more equal share between

120 coccolithophores and foraminifers today (Schiebel, 2002) raise questions about the

121 potential impact on bulk carbonate derived isotopes. Combined with the geographic

122 differences in their importance for carbonate production and the differential

123 preservation potential of the two main carbonate producers it is imperative to assess the

124 importance of these processes on Li isotope composition.

125   We examine the Li isotope composition of core tops from several different

126   geographic locations in the Atlantic, as well as some shallow-water aragonitic sites

127   from the Bahamas. The aim is to determine whether bulk carbonate is a viable archive

128   for seawater Li isotopes, and if not, to determine the circumstances when it is not.

129

130   2.0 Samples

131   The Atlantic core-top samples used are largely taken from Geo Bremen cruises

132   of the research vessel RV Meteor between 1988 and 2000. The samples span the North

133   and South Atlantic from 70° north to 44° south (Fig. 1), relatively close to the shore

134   (~50km in the sample GeoB 11024-1 from the Galician continental margin, and ~180

135   km in the S. Atlantic sample 1719-5), as well as deep ocean sites. We also examine a

136   decarbonated samples from the Ocean Drilling Programme Site 980, on the Feni Drift

137   in the NE Atlantic, and a clay sample from GeoB 6409-2 from the central South

138   Atlantic. Sample depths range from 930 to 5389 m below sea-level (Table 1 and 2).

139   Of the 16 core-tops analysed, 7 consist largely of foraminiferal ooze with other

140   common carbonate particles and some opaline components, such as diatoms (Table 3).

141   Five core-tops (Table 3) contain optically trace amounts of aragonite, while two further

142   ones (GeoB 1724-3 and GeoB 11024-1) dominantly consist of quartz grains, with only

143   relatively little carbonate. These two latter core-tops were analysed to test whether

144   sections with trace-level carbonate (<10%) are still a viable seawater archive.

145   The Bahamian surface samples were collected from a several km^2 area near the

146   Exuma Cays on the eastern side of the Great Bahama Bank (Fig. 2), which is typically

147   considered the 'type' modern shallow water carbonate depositional analogue (Schlager

148   and Ginsburg, 1981). This relatively small geographic area in the Bahamas provides

149   multiple facies and different carbonate factories. This region has been used previously

150   to study B and U isotope behaviour in shallow water carbonates (Romaniello et al.,

151   2013; Zhang et al., 2017). Depth of the samples ranged from roughly 2–12 meters, with

152   depth varying on a daily basis with the tides. There is rapid exchange of water with tidal

153   cycles in the Exumas, with Atlantic surface water coming onto the bank-top and warmer

154   and slightly more saline waters coming off the bank-top. There have been multiple

155   papers describing the sediments and marine cements present in Exumas (Ginsburg and

156   Planavsky, 2008; Planavsky and Ginsburg, 2009; Whittle et al., 1993) and, therefore,

157   we provide only a brief description of the environment and samples. The sediment types

158   and environmental setting for each sample are listed in Table 2. Sediment grain size

159   varies from predominantly micrite (carbonate mud) to coarse grainstones. All

160   sediments are dominated by aragonite, but there may be trace amounts of high and low

161   Mg calcite (Zhang et al., 2017). The fine-grained material is typically derived from

162   green algae whereas the grainstones are a mix of algae and metazoan clasts and

163   nonskeletal grains (Wright and Burgess, 2005) We also analysed a marine hardground

164   and a stromatolite, which in the Bahamas are basically peloidal grainstones cemented

165   together (predominantly by botryoidal aragonite cements (Ginsburg and Planavsky,

166   2008)).

167

168   3.0 Methods

169   To determine the relative importance of coarse versus fine carbonate material,

170   which in the open ocean approximates the contribution of foraminifers versus

171   coccolithophores, bulk samples were washed and filtered at 20 microns. The carbonate

172   content (weight percent) of each sample was calculated based on total carbon (TC) and

173   total organic carbon (TOC) contents measured using a LECO-CS 200 element analyzer.

174   The calculation was made according to the equation $CaCO_3\% = 8.33*(TC\% - TOC\%)$.

175   X-ray diffraction analysis was used to determine aragonite contents in two of the

176   samples. The sand fraction > 63 μm was analysed microscopically for major sediment

177   contributors. The decarbonated sample was treated by addition of 12.5g HCl.

178   For the Atlantic samples the exchangeable fraction of the samples was leached

179   using 1M sodium acetate for 1 hour at room temperature (Tessier et al., 1979). The bulk

180   carbonate fraction of the samples was leached by two different methods. The first used

181   0.1M HCl for 1 hour at room temperature (Pogge von Strandmann et al., 2013). This

182   method has the advantage that no additional cation matrix is added to the sample, but

183   the potential drawback of using a strong acid is that any silicate fraction could also be

184   leached. Therefore, we also used a Tessier leaching method, where acetic acid was

185   buffered with sodium acetate to pH5 (Tessier et al., 1979). This method should attack

186   silicates less, but has the disadvantage of adding significant amounts of Na to the

187   sample, which the cation exchange columns have to deal with.

188   In both cases, the leached carbonate samples were analysed for trace element

189   ratios using a quadrupole ICP-MS, with calibration standards and samples matrix-

190   matched to 10 μg/g Ca (and also to Na content in the case of Na-acetate leaches). This

191   is important to determine whether silicates have been inadvertently leached, by

192   examining ratios such as Al/Ca and Mn/Ca (Pogge von Strandmann et al., 2013). The

193   international reference standard JLs-1 was used to assess accuracy and precision, which

194   is within 5% for all elements analysed.

195   The residual fractions (after the exchangeable and carbonate fractions were

196   removed) were dissolved in concentrated $HF-HNO_3-HClO_4$, followed by concentrated

197   HNO_3 and 6M HCl.

198   Lithium isotopes of the Atlantic samples were purified using a two-step cation

199   exchange method, which has been detailed for carbonates in numerous studies (Pogge

200   von Strandmann et al., 2017a; Pogge von Strandmann and Henderson, 2015; Pogge von

201   Strandmann et al., 2013). Analyses were performed on a Nu Instruments HR MC-ICP-

202   MS at the University of Oxford. Secondary standards run include seawater (δ^7Li = 31.3

203   ± 0.6‰, 2sd, n=62), USGS basalt BCR-2 (δ^7Li = 2.6 ± 0.5‰, 2sd, n=5) and shale SGR-

204   1 (δ^7Li = 3.6 ± 0.4‰, 2sd, n=3). SGR-1 was also leached for its carbonate and residual

205   fractions. The residual and bulk δ^7Li values of SGR-1 are identical (3.5 vs. 3.4‰,

206   respectively). Repeats of the samples analysed here also reproduce with an uncertainty

207   of ±0.6‰ (Table 1 and 2).

208   For the Bahamian samples the exchangeable fraction was removed with a

209   roughly one hour 1M ammonium acetate leach. The carbonate was dissolved in 0.05 M

210   HCl. Concentration analyses on the carbonate leaches were performed using a Thermo

211   Finnigan Element XR. Analytical uncertainty was less than 5% based on sample

212   duplicates and measurements of the USGS standard BHVO. A sample split of the acid

213   digest was brought up in 0.2N HCl and loaded Bio-Rad AG50W-X12 (200-400 mesh)

214   cation exchange resin pre-cleaned with 6N HCl. Matrix elements were eluted with 0.2N

215   HCl and then Li was eluted with 0.5N HCl (Dellinger et al., 2017). Li and Na

216   concentrations were analysed after column work, prior to Li isotope analysis. The Li

217   and Na post-column concentrations and the Li isotopic composition were measured

218   with a Thermo Finnigan Neptune Plus MC-ICP-MS at Yale Metal Geochemistry Center

219   using an ESI Apex-IR desolvating nebulizer. Li isotope data was collected at low

220   resolution in 1 block with 50 cycles per block. L-SVEC standard and an in-house Li

221   solution (δ^7Li = 43.5‰ ± 0.31‰ relative to L-SVEC, 2sd, n = 50) was used to monitor

222   the long-term reproducibility of Li isotope analyses. The overall reproducibility and

223   accuracy of the Li procedure (sample digestion, Li separation, and Li isotope analysis)

224   were checked by repeated measurements of OSIL seawater (δ^7Li = 30.7‰ ± 0.5‰

225 relative to L-SVEC, 2sd, n = 7) and BHVO-2 (δ^7Li = 4.4‰ ± 0.3‰ relative to L-SVEC,

226 2sd, n = 7 digestions).

227

228 <u>4.0 Results</u>

229 *4.1 Atlantic Core-tops*

230   Examination of the carbonate mineralogy of the samples shows that the bulk

231 CaCO$_3$ composition varies between ~4 and 85%, and total organic carbon between ~0.2

232 and 2.4% (Table 3). At least one sample (GeoB 4315-1) also contains significant

233 (~17%) aragonite. By means of the bulk carbonate >20μm CaCO$_3$ data and the

234 proportion of that grain size in the total sediment (Table 3), it is possible to calculate

235 the foraminifer carbonate content in the total sediment, and then assume that the

236 difference is coccolith carbonate (<20μm). As shown in Table 3, some samples are

237 dominated by foraminiferal carbonate, while others are more dominated by coccolith

238 carbonate.

239   The exchangeable fraction's δ^7Li for all samples ranges between 13.8 and

240 16.7‰, with the clay samples' exchangeable δ^7Li within that range (14.2–14.4‰). The

241 resulting Δ^7Li$_{seawater-exch}$ is 14.6–17.5‰, close to the theoretical value of 15–16‰ of

242 authigenic clays required to balance seawater δ^7Li (Chan et al., 1992; Hathorne and

243 James, 2006; Misra and Froelich, 2012).

244   Carbonate leaches have δ^7Li ranging between 10.5 and 26.8‰, with no

245 relationship between δ^7Li and the fraction of carbonate in the sample or total organic

246 carbon (Table 1). The carbonate leach of SGR-1 also has a δ^7Li of 22.4‰. Generally,

247 the Al/Ca and Mn/Ca of the HCl leaches are higher than those of the Na acetate leaches

248 (Table 1), although all are below the calculated nominal cutoff value above which

249 silicate Li would begin to affect total δ^7Li (Pogge von Strandmann et al., 2013).

250   Generally, the δ^7Li values of both leaches are similar for each sample, with the average

251   difference 0.11‰, and a maximum difference of 2.6‰ (Fig. 3).

252   The silicate residues have δ^7Li values of -1.8 to 2.6‰, with an average of 0.8‰,

253   generally similar to the values of the upper continental crust (Sauzéat et al., 2015), and

254   to marine sediments (Chan et al., 2006). The Li concentrations in these fractions are

255   quite variable (4.1–72 μg/g), and between 2.3 and 36% of total Li in these samples is

256   located in the carbonate fractions, clearly demonstrating how important a clean leach

257   of the carbonate fraction is.

258

259   *4.2 Bahamas surface samples*

260   The Bahamian aragonite samples have a relatively narrow range in Li/Ca (18.6

261   ± 4 μmol/mol) (Table 1). As would be expected, given aragonite minerology, their

262   Sr/Ca is also significantly higher than the dominantly calcitic core-tops: ~10±1

263   mmol/mol, compared to ~1.5 mmol/mol in the core-tops. The δ^7Li varies between 20.2

264   and 22.5‰, and the average $\Delta^7Li_{seawater-arag} = 9.6 \pm 0.6$‰.

265

266   <u>5.0 Discussion</u>

267   *5.1 Bahamas samples*

268   There is no correlation between elemental ratios such as Li/Ca, Mg/Ca or Sr/Ca

269   and the narrow range in δ^7Li in these samples. The key observation from these entirely

270   aragonitic samples is that the $\Delta^7Li_{seawater-sample}$ of 9.6 ± 0.6‰ (Fig. 4) is within the range

271   shown for inorganic aragonites (11.7 ± 0.5‰ (Marriott et al., 2004b)), given the ±1.0‰

272   uncertainty of the latter study. Biogenic aragonites, from molluscs (clams) and corals,

273   exhibit a wider scatter of ~8–16‰ (Dellinger et al., 2018; Marriott et al., 2004a;

274   Rollion-Bard et al., 2009). Therefore, this study's bulk aragonites exhibit a very narrow

275   range in Δ^7Li, which is entirely consistent with inorganic and biogenic aragonites (Fig.

276   4). Samples from this area have shown variations in boron isotopes between different

277   carbonate types (e.g. ooids, cements, carbonate muds and micrite (Zhang et al., 2017)),

278   which is thought to result from microbially-mediated carbonate precipitation. The

279   relative invariance of our Li isotope data suggest that, in aragonites at least, the Li

280   isotope fractionation factor is relatively constant in all these different carbonate types.

281   Assuming limited diagenetic effects, it appears that bulk aragonites can be used to track

282   past seawater δ^7Li values.

283

284   *5.2 Core-top Li/Ca ratios*

285   The Li/Ca ratios of the core-top carbonate leaches ranges between 21 and 71

286   μmol/mol. There is no trend between Li/Ca and the proportion or weight of the fine vs.

287   the coarse carbonate fraction, suggesting no trend with the foraminifer to coccolith

288   ratio. However, the Li/Ca range of samples that are dominated by foraminiferal ooze

289   (average 25 μmol/mol) are only slightly higher then modern and Holocene foraminifera

290   (<18.5 (Hall and Chan, 2004; Hathorne and James, 2006; Marriott et al., 2004b; Misra

291   and Froelich, 2009). In contrast, samples that are largely agglutinated abiotic carbonate,

292   combined with aragonites and other particles (Table 3), tend to have higher Li/Ca ratios,

293   averaging ~34 μmol/mol. Some biogenic carbonates have much higher Li/Ca values,

294   with molluscs ranging from ~20–60 μmol/mol and high-Mg calcites, such as

295   echinoderms, with values close to 100 μmol/mol (Dellinger et al., 2018). In contrast,

296   benthic foraminifera, corals and aragonitic molluscs have Li/Ca values of ~2–20

297   μmol/mol (Dellinger et al., 2018). Bulk carbonates from the geologic record have Li/Ca

298   ratios that have a larger spread from 0.9 to 46 μmol/mol (Lechler et al., 2015; Pogge

299   von Strandmann et al., 2017a; Pogge von Strandmann et al., 2013). Hence, the type of

300   carbonate mineralogy and the mixture of calcifying organisms is likely controlling

301   significant parts of the variation in Li/Ca. The two samples dominated by quartz, with

302   only little carbonate, have an average of ~59 µmol/mol. This is unlikely to stem directly

303   from leaching of quartz or opal, because ratios such as Al/Ca, Mn/Ca and Sr/Ca are still

304   low. However, it is possible that cation exchange occurred between the silicates and

305   trace carbonates, increasing the concentration of some elements, especially Li.

306   Early stage diagenesis in carbonates is sometimes monitored by comparing

307   Sr/Ca ratios to Mn or Mn/Ca, where diagenesis should decrease Sr/Ca and increase Mn

308   (Korte et al., 2005; van Geldern et al., 2006). In our samples, there is no trend between

309   Sr/Ca (or Li/Ca) and Mn/Ca or δ^7Li. Further, Sr/Ca ratios are uniformly higher than

310   nominally diagenetic cutoff values (Brand and Veizer, 1980; Korte et al., 2005),

311   suggesting that these samples have not been resolvably diagenetically perturbed.

312   There is no simple trend in our carbonates with latitude (Fig. 6), suggesting no

313   direct controlling influence by temperature, nor with depth (Fig. 7), although inorganic

314   carbonate Li/Ca ratios are inversely correlated with temperature, with values decreasing

315   by a factor of ~3 for a 30°C increase in temperature (Marriott et al., 2004a; Marriott et

316   al., 2004b). This may suggest that there is an overarching biological control on Li/Ca,

317   especially given that more Li/Ca variation exists at high latitudes, which may mean that

318   there is a secondary control on Li/Ca, via a temperature and location control on the

319   types of carbonate growing in those waters (Fig. 6).

320   There is also no obvious offset in Li/Ca (or Sr/Ca) in core-top samples that have

321   aragonite, compared to those that do not (Fig. 6), in contrast to the pure aragonitic

322   samples from the Bahamas. The geographic difference of the aragonite saturation

323   horizon in the Atlantic with higher saturation in the North Atlantic than the South

324   Atlantic (Jiang et al., 2015) should have resulted in a geographic bias if the trace

325 amounts of aragonite in these core-tops would significantly affect the bulk mass

326 balance. Hence, in detail, elemental ratios are likely to be controlled by the mix of

327 carbonate mineralogy and biogenic carbonate producer at each site, modified by

328 external parameters such as temperature. This is not unexpected, and highlights why

329 foraminifera are generally the archive of choice for reconstruction of past Li/Ca ratios

330 (Lear et al., 2010; Lear and Rosenthal, 2006).

331

332 *5.3 Core-top exchangeable fractions*

333   In principle, Li from seawater will be adsorbed onto the exchangeable fraction,

334 with an inherent isotope fractionation. Whether there is a fractionation difference

335 between adsorbed and structurally bound Li in silicate clays has never been fully

336 addressed. There is potentially a mineralogical effect on the fractionation factor (Millot

337 and Girard, 2007; Pistiner and Henderson, 2003; Vigier et al., 2009; Wimpenny et al.,

338 2015; Wimpenny et al., 2010), although the minerals withdrawing Li from seawater by

339 sorption are expected to have a broadly similar fractionation as during authigenic clay

340 neoformation, of ~15‰ (Chan et al., 1992; Hathorne and James, 2006; Pogge von

341 Strandmann et al., 2008).

342   The data from the core-top exchangeable fractions leached during this study

343 suggest a narrow range in δ^7Li, on average 16.5 ± 0.8‰ lower than seawater (Fig. 8).

344 The exchangeable fraction from the decarbonated sample has a similar δ^7Li (~14‰),

345 suggesting that the exchangeable sites in all samples are on the silicate portion of each

346 sample. In other words, there is apparently no exchangeable uptake onto carbonate

347 surfaces, or if there is, it imposes the same fractionation factor.

348   Another unknown factor in the behaviour of lithium in the oceans is how much

349 Li is taken up into exchangeable sites. Mass balance of Li in the exchangeable leach

350   compared to the residual and carbonate samples suggests that 2.0±0.6% is sorbed onto

351   silicate exchangeable sites. This is approximately a factor of four less Li than is being

352   taken into carbonates in these samples, suggesting that sorbed Li is an insignificant sink

353   from the global oceans. Until laboratory experiments are conducted, though, it will be

354   unknown how long the exchangeable isotope ratio can be preserved for, and hence

355   whether this phase can be used as an archive of past seawater δ^7Li values.

356

357   *5.4 Core-top carbonate fractions*

358   Generally, the two different carbonate leaching methods employed yield the

359   same δ^7Li values. There are some samples where the difference between the two

360   leaches is up to ~2.5‰, easily resolvable outside of analytical uncertainty. In most of

361   these cases, the Na acetate leach is isotopically heavier, and has slightly lower Al/Ca,

362   Mn/Ca and Li/Ca values. Given that leaching of silicates would drive δ^7Li lower and

363   element/Ca ratios higher, it seems likely that the difference in δ^7Li is due to the addition

364   of Li (and other elements) leached from silicates during attack with dilute HCl.

365   Therefore, while the values are generally similar (Fig. 3), leaching with Na acetate is

366   likely a more robust method for attaining Li from the carbonate fraction only.

367   In samples that contain no aragonite, the $\Delta^7Li_{seawater-carbonate}$ is 6.1 ± 1.3‰ (2sd)

368   (Fig. 5). There is no trend with latitude or ocean depth similar to the Li/Ca ratio (Fig.

369   7). This isotopic range is similar to the range suggested by inorganic calcite

370   precipitation from seawater of ~3–5‰ (Marriott et al., 2004b), albeit those experiments

371   used Li concentrations ~10 times higher than seawater. The fractionation factor

372   observed is less than calcite grown from pure water without other trace elements (~8‰

373   (Marriott et al., 2004a)). Planktic foraminifera exhibit a species-specific fractionation

374   factor of 0–4‰ (Hall et al., 2005; Hathorne and James, 2006), while benthic

375　foraminifera (*Uvigerina* spp.) show fractionation of 4–10‰ (Marriott et al., 2004b).

376　Brachiopods incur ~3.5–5.5‰ fractionation (Dellinger et al., 2018). In contrast,

377　molluscs, especially oysters, are highly variable, with $\Delta^7Li_{seawater-carbonate}$ ~ -10 to +8‰,

378　with large differences within even mono-mineralic shells, thought to be due to both

379　environmental and calcification effects (Dellinger et al., 2018). Overall, our relatively

380　deep marine samples are within the ranges for inorganic and foraminiferal calcite, albeit

381　with a slightly higher average. There is also no relationship between δ^7Li (or Li/Ca)

382　and the % the fine fraction makes up of each sample (Table 3), which can be used as a

383　first order approximation of the ratio of foraminifera to coccoliths.

384　　　　In comparison, inorganic aragonite imparts a higher fractionation of $\Delta^7Li_{seawater-}$

385　$_{carbonate}$ ~ 11‰ (Marriott et al., 2004b), similar to our Bahamian aragonitic samples.

386　Equally, aragonitic molluscs and corals impart greater fractionation of 8–16‰

387　(Dellinger et al., 2018). Our core-top carbonate samples that contain some aragonite

388　(Table 3) have a much greater Δ^7Li variability of 4.7 to 20.3‰, albeit this range is

389　dominated by the exceptionally light and anomalous sample from the Galician coast

390　discussed below. The Atlantic samples with trace aragonite range from 4.7 to 6.4‰

391　(average 5.4 ± 0.7‰), effectively indistinguishable from the calcitic samples. This is

392　not necessarily unexpected, given the only trace levels of aragonite. Sample GeoB4315-

393　1, however, contains around 17% aragonite, and exhibits a $\Delta^7Li_{seawater-carbonate} = 6.1‰$.

394　Assuming the observed average distribution of Li between calcite and aragonite, and

395　their fractionation factors, this proportion should yield a fractionation of ~6.7‰, within

396　uncertainty of that observed. Hence, the presence of aragonite can perturb the carbonate

397　δ^7Li, but in these core-top samples the proportion of aragonite to calcite is too small to

398　have a significant effect. Extrapolating this mass balance suggests that the aragonite

399　content would have to be >35% before the bulk Δ^7Li composition would be resolvably

400   affected. Modern open marine sediments are consistently dominated by calcite, and

401   rarely have >10% aragonite, meaning that open marine core-tops should consistently

402   be uniformly isotopically offset from seawater.

403   Two of our core-top samples (GeoB1724-4 and 11024-1) predominantly consist

404   of quartz, with some volcanic ash and opaline organisms, and were analysed to test

405   whether trace carbonates in sections are still viable seawater archives. The former

406   sample has a "normal' calcite δ^7Li value, whereas the latter has the lowest δ^7Li

407   measured here. 1724-4 contains some detrital carbonate, and, given the low Al/Ca and

408   Mn/Ca ratios and carbonate-like δ^7Li, it seems likely that this was the only phase

409   leached by the Na acetate method. Thus, this leaching method appears to be able to be

410   applied to some modern very carbonate-poor samples (4.2% carbonate).

411   Sample 11024-1 is from the Galician continental margin, and has δ^7Li values of

412   ~11‰. This sample also exhibits higher Li/Ca than other samples (Fig. 6). Given that

413   the sample also has low Al/Ca, these higher Li/Ca values are unlikely to stem from

414   silicate dissolution. The Δ^7Li value of ~20‰ is considerably greater than even from the

415   pure aragonitic Bahamian samples, and therefore additional processes must be lowering

416   the δ^7Li. While very low δ^7Li values (~5‰) have been reported from the (radiolarian-

417   rich) core-top carbonates of ODP Site 851B (eastern equatorial Pacific) (You et al.,

418   2003), no trace element data were included in that study, and hence it is possible that

419   radiolarian silicates were partially leached, lowering the bulk δ^7Li.

420   There are therefore two possibilities to explain the low δ^7Li in the sample from

421   the Galician coast: 1) recrystallisation of the carbonate and incorporation of Li from the

422   silicate fraction; 2) localised incorporation of Li from anthropogenic sources such as

423   fertiliser, given this is a relatively near-shore site. The latter possibility is unlikely,

424   however, given that this is still an open ocean site. We note that this sample has the

425 highest proportion of Li in silicates relative to carbonates (only ~2.3% of the total Li is

426 in the carbonate fraction). Data from such carbonate-poor samples must therefore be

427 treated with a degree of caution when reconstructing past seawater δ^7Li.

428

429 <u>6.0 Conclusions</u>

430   In this study we determined the bulk Li isotope composition of carbonate from

431 27 Bahamian aragonitic samples, and the exchangeable, carbonate and residual phases

432 for Li isotopes of 16 Atlantic core-top sediments, to determine whether bulk carbonates

433 can serve as a reliable archive of seawater Li isotope ratios.

434   Around 2% of the total Li is situated in the exchangeable fractions, which has a

435 ~16.5‰ fractionation from seawater. Carbonate leaching techniques using dilute HCl

436 and acetic acid buffered with Na acetate are compared. While δ^7Li values are similar,

437 the Na acetate method yields slightly lower Al/Ca and Mn/Ca values and higher δ^7Li.

438 These results suggest that the HCl method can weakly leach the silicate fractions of the

439 sediments. We therefore recommend that bulk carbonates, if there is siliciclastic

440 material in the sample, are leached using acetic acid buffered with Na acetate.

441   Bulk carbonate samples that only contain calcite have a uniform and constant

442 offset from seawater of Δ^7Li$_{seawater-carbonate}$ = 6.1 ± 1.3‰ (2sd), close to that exhibited by

443 inorganic and several biogenic calcites. Five core-tops contain trace amounts of

444 aragonite, but exhibit no difference in their Δ^7Li$_{seawater-carbonate}$. Mass balance agrees with

445 our analyses, and that even the most aragonite-rich core-top, with 17% aragonite, would

446 only see 0.6‰ more fractionation due to this difference in mineralogy when compared

447 to a pure calcite sample.

448   In contrast, the pure aragonite samples from the Bahamas have Δ^7Li$_{seawater-}$

449 $_{carbonate}$ = 9.6 ± 0.6‰, in keeping with inorganic aragonite fractionation experiments.

450   Two core-top samples have <10% carbonate contents, and were analysed to test

451   whether trace carbonates are still a viable seawater archive. The calcite in one of these

452   samples (GeoB 1724-4) has a similar carbonate δ^7Li to the carbonate-rich core-tops,

453   while the other sample (from the Galician coast) has a very low carbonate δ^7Li

454   ($\Delta^7Li_{seawater-carbonate}$ = 20‰) that cannot be explained by any known carbonate

455   fractionation factors. This sample also has slightly higher Li/Ca values and could be

456   explained either by localised addition of anthropogenic Li, or, more likely by

457   recrystallisation of the carbonate, gaining Li from the silicate portion, which in this

458   sample is particularly enriched in Li.

459   Overall, core-top bulk carbonates (both calcites and aragonites) from the open

460   ocean are a reliable archive for seawater δ^7Li. The lack of correlation between bulk

461   carbonate δ^7Li and latitude, depth or carbonate make-up suggests that bulk carbonates

462   may be a more robust archive than foraminifera, where vital effects may complicate the

463   signal. However, care must be taken concerning carbonate mineralogy, in that the

464   original carbonate type must be known before attempting to reconstruct seawater δ^7Li

465   values. The potential effects of carbonate-poor samples must also be determined.

466   Overall using bulk carbonates as archives of palaeo-seawater δ^7Li clearly has high

467   potential, but it must be stressed that any values should be reproduced in different global

468   sections, to avoid small mineralogical effects, or potentially larger effects of cation

469   exchange.

470

471

477

478

479 Berner, R.A., 2003. The long-term carbon cycle, fossil fuels and atmospheric
480   composition. Nature, 426(6964): 323-326.
481 Brand, U., Veizer, J., 1980. Chemical diagenesis of a multicomponent carbonate
482   system: 1. Trace elements. Journal of Sedimentary Petrology, 50: 1219–
483   1236.
484 Chamberlin, T.C., 1899. An attempt to frame a working hypothesis of the cause of
485   glacial periods on an atmospheric basis. Journal of Geology, 7(6): 545–
486   584.
487 Chan, L.H., Edmond, J.M., 1988. Variation of lithium isotope composition in the
488   marine environment: A preliminary report. Geochimica Et Cosmochimica
489   Acta, 52: 1711–1717.
490 Chan, L.H., Edmond, J.M., Thompson, G., Gillis, K., 1992. Lithium isotopic
491   composition of submarine basalts: implications for the lithium cycle in the
492   oceans. Earth and Planetary Science Letters, 108(1-3): 151-160.
493 Chan, L.H., Gieskes, J.M., You, C.F., Edmond, J.M., 1994. Lithium isotope
494   geochemistry of sediments and hydrothermal fluids of the Guaymas
495   Basin, Gulk of California. Geochimica Et Cosmochimica Acta, 58: 4443-
496   4454.
497 Chan, L.H., Leeman, W.P., Plank, T., 2006. Lithium isotopic composition of marine
498   sediments. Geochemistry Geophysics Geosystems, 7: Q06005.
499 Dellinger, M., Bouchez, J., Gaillardet, J., Faure, L., Moureau, J., 2017. Tracing
500   weathering regimes using the lithium isotope composition of detrital
501   sediments. Geology, in press.
502 Dellinger, M. et al., 2015. Riverine Li isotope fractionation in the Amazon River
503   basin controlled by the weathering regimes. Geochimica Et Cosmochimica
504   Acta, 164: 71–93.
505 Dellinger, M. et al., 2018. The Li isotope composition of marine biogenic
506   carbonates: Patterns and mechanisms. Geochimica Et Cosmochimica Acta,
507   in press.
508 Elliott, T., Thomas, A., Jeffcoate, A., Niu, Y.L., 2006. Lithium isotope evidence for
509   subduction-enriched mantle in the source of mid-ocean-ridge basalts.
510   Nature, 443(7111): 565–568.
511 Fantle, M.S., Tipper, E.T., 2014. Calcium isotopes in the global biogeochemical Ca
512   cycle: Implications for development of a Ca isotope proxy. Earth-Science
513   Reviews, 129: 148–177.
514 Ginsburg, R.N., Planavsky, N.J., 2008. Diversity of Bahamian Microbialite
515   Substrates. In: Dilek, Y., Furnes, H., Muehlenbacks, K. (Eds.), Links
516   Between Geological Processes, Microbial Activities & Evolution of Life.
517   Modern Approaches in Solid Earth Sciences. Springer, Dordrecht

518 Hall, J.M., Chan, L.H., 2004. Li/Ca in multiple species of benthic and planktonic
519   foraminifera: Thermocline, latitudinal, and glacial-interglacial variation.
520   Geochimica Et Cosmochimica Acta, 68(3): 529–545.
521 Hall, J.M., Chan, L.H., McDonough, W.F., Turekian, K.K., 2005. Determination of the
522   lithium isotopic composition of planktic foraminifera and its application
523   as a paleo-seawater proxy. Marine Geology, 217(3-4): 255–265.
524 Hathorne, E.C., James, R.H., 2006. Temporal record of lithium in seawater: a
525   tracer for silicate weathering? Earth and Planetary Science Letters, 246:
526   393–406.
527 Hawley, S.M., Pogge von Strandmann, P.A.E., Burton, K.W., Williams, H.M.,
528   Gislason, S.R., 2017. Continental weathering and terrestrial
529   (oxyhydr)oxide export: Comparing glacial and non-glacial catchments in
530   Iceland. Chemical Geology, 462: 55–66.
531 Huh, Y., Chan, L.H., Edmond, J.M., 2001. Lithium isotopes as a probe of weathering
532   processes: Orinoco River. Earth and Planetary Science Letters, 194(1-2):
533   189–199.
534 Huh, Y., Chan, L.H., Zhang, L., Edmond, J.M., 1998. Lithium and its isotopes in
535   major world rivers: Implications for weathering and the oceanic budget.
536   Geochimica Et Cosmochimica Acta, 62(12): 2039–2051.
537 Jiang, L.-Q., Feely, R.A., Carter, B.R., Greeley, D.J., Gledhill, D.K., 2015.
538   Climatological distribution of aragonite saturation state in the global
539   oceans. Global Biogeochemical Cycles, 29: 1656–1673.
540 Kisakürek, B., James, R.H., Harris, N.B.W., 2005. Li and δ^7Li in Himalayan rivers:
541   Proxies for silicate weathering? Earth and Planetary Science Letters,
542   237(3-4): 387–401.
543 Korte, C., Kozur, H.W., Veizer, J., 2005. δ^{13}C and δ^{18}O values of Triassic
544   brachiopods and carbonate rocks as proxies for coeval seawater and
545   palaeotemperature. Palaeogeography Palaeoclimatology Palaeoecology,
546   226: 287–306.
547 Lear, C.H., Mawbey, E.M., Rosenthal, Y., 2010. Cenozoic benthic foraminiferal
548   Mg/Ca and Li/Ca records: Toward unlocking temperatures and saturation
549   states. Paleoceanography, PA4215.
550 Lear, C.H., Rosenthal, Y., 2006. Benthic foraminiferal Li/Ca: Insights into Cenozoic
551   seawater carbonate saturation state. Geology, 34(11): 985–988.
552 Lechler, M., Pogge von Strandmann, P.A.E., Jenkyns, H.C., Prosser, G., Parente, M.,
553   2015. Lithium-isotope evidence for enhanced silicate weathering during
554   OAE 1a (Early Aptian Selli event). Earth and Planetary Science Letters,
555   432: 210–222.
556 Lemarchand, E., Chabaux, F., Vigier, N., Millot, R., Pierret, M.C., 2010. Lithium
557   isotope systematics in a forested granitic catchment (Strengbach, Vosges
558   Mountains, France). Geochimica Et Cosmochimica Acta, 74: 4612-4628.
559 Marriott, C.S., Henderson, G.M., Belshaw, N.S., Tudhope, A.W., 2004a.
560   Temperature dependence of δ^7Li, δ^{44}Ca and Li/Ca during growth of
561   calcium carbonate. Earth and Planetary Science Letters, 222: 615–624.
562 Marriott, C.S., Henderson, G.M., Crompton, R., Staubwasser, M., Shaw, S., 2004b.
563   Effect of mineralogy, salinity, and temperature on Li/Ca and Li isotope
564   composition of calcium carbonate. Chemical Geology, 212(1-2): 5–15.

565 Millot, R., Girard, J.P., 2007. Lithium Isotope Fractionation during adsorption
566   onto mineral surfaces, International meeting, Clays in natural &
567   engineered barriers for radioactive waste confinement, Lille, Frace.
568 Millot, R., Vigier, N., Gaillardet, J., 2010. Behaviour of lithium and its isotopes
569   during weathering in the Mackenzie Basin, Canada. Geochimica Et
570   Cosmochimica Acta, 74: 3897–3912.
571 Misra, S., Froelich, P.N., 2009. Measurement of lithium isotope ratios by
572   quadrupole-ICP-MS: application to seawater and natural carbonates.
573   Journal of Analytical Atomic Spectrometry, 24(11): 1524-1533.
574 Misra, S., Froelich, P.N., 2012. Lithium Isotope History of Cenozoic Seawater:
575   Changes in Silicate Weathering and Reverse Weathering. Science, 335:
576   818–823.
577 Oliver, L. et al., 2003. Silicate weathering rates decoupled from the $^{87}Sr/^{86}Sr$ ratio
578   of the dissolved load during Himalayan erosion. Chemical Geology, 201(1-
579   2): 119–139.
580 Opfergelt, S. et al., 2010. Variations of δ30Si and Ge/Si With Weathering and
581   Biogenic Input in Tropical Basaltic Ash Soils Under Monoculture.
582   Geochimica Et Cosmochimica Acta, 74: 225-240.
583 Pistiner, J.S., Henderson, G.M., 2003. Lithium-isotope fractionation during
584   continental weathering processes. Earth and Planetary Science Letters,
585   214(1-2): 327-339.
586 Planavsky, N.J., Ginsburg, R.N., 2009. Taphonomy of modern marine Bahamian
587   microbialites. Palaios, 24: 5–17.
588 Pogge von Strandmann, P.A.E., Burton, K.W., James, R.H., van Calsteren, P.,
589   Gislason, S.R., 2010. Assessing the role of climate on uranium and lithium
590   isotope behaviour in rivers draining a basaltic terrain. Chemical Geology,
591   270: 227–239.
592 Pogge von Strandmann, P.A.E. et al., 2006. Riverine behaviour of uranium and
593   lithium isotopes in an actively glaciated basaltic terrain. Earth and
594   Planetary Science Letters, 251: 134–147.
595 Pogge von Strandmann, P.A.E. et al., 2016. The effect of hydrothermal spring
596   weathering processes and primary productivity on lithium isotopes: Lake
597   Myvatn, Iceland. Chemical Geology, 445: 4–13.
598 Pogge von Strandmann, P.A.E. et al., 2017a. Global climate stabilisation by
599   chemical weathering during the Hirnantian glaciation. Geochemical
600   Perspective Letters, 3: 230–237.
601 Pogge von Strandmann, P.A.E., Forshaw, J., Schmidt, D.N., 2014. Modern and
602   Cenozoic records of seawater magnesium from foraminiferal Mg isotopes.
603   Biogeosciences, 11: 5155–5168.
604 Pogge von Strandmann, P.A.E., Frings, P.J., Murphy, M.J., 2017b. Lithium isotope
605   behaviour during weathering in the Ganges Alluvial Plain. Geochimica Et
606   Cosmochimica Acta, 198: 17–31.
607 Pogge von Strandmann, P.A.E., Henderson, G.M., 2015. The Li isotope response to
608   mountain uplift. Geology, 43(1): 67–70.
609 Pogge von Strandmann, P.A.E., James, R.H., van Calsteren, P., Gíslason, S.R.,
610   Burton, K.W., 2008. Lithium, magnesium and uranium isotope behaviour
611   in the estuarine environment of basaltic islands. Earth and Planetary
612   Science Letters, 274(3-4): 462-471.

613   Pogge von Strandmann, P.A.E., Jenkyns, H.C., Woodfine, R.G., 2013. Lithium
614   isotope evidence for enhanced weathering during Oceanic Anoxic Event 2.
615   Nature Geoscience, 6: 668–672.
616   Roberts, J. et al., 2018. Lithium isotopic composition of benthic foraminifera: A
617   new proxy for paleo-pH reconstruction. Geochimica Et Cosmochimica
618   Acta, 236: 336–350.
619   Rollion-Bard, C. et al., 2009. Effect of environmental conditions and skeletal
620   ultrastructure on the Li isotopic composition of scleractinian corals. Earth
621   and Planetary Science Letters, 286: 63–70.
622   Romaniello, S.J., Hermann, A.D., Anbar, A.D., 2013. Uranium concentrations and
623   238U/235U isotope ratios in modern carbonates from the Bahamas:
624   Assessing a novel paleoredox proxy. Chemical Geology, 362: 305–316.
625   Sauzéat, L., Rudnick, R.L., Chauvel, C., Garcon, M., Tang, M., 2015. New
626   perspectives on the Li isotopic composition of the upper continental crust
627   and its weathering signature. Earth and Planetary Science Letters, 428:
628   181–192.
629   Schiebel, R., 2002. Planktic foraminiferal sedimentation and the marine calcite
630   budget. Global Biogeochemical Cycles, 16.
631   Schlager, W., Ginsburg, R.N., 1981. Bahama carbonate platforms — The deep and
632   the past. Marine Geology, 44: 1–24.
633   Tessier, A., Campbell, P.G.C., Bisson, M., 1979. Sequential Extraction Procedure
634   for the Speciation of Particulate Trace Metals. Analytical Chemistry, 51(7):
635   844-851.
636   Ullmann, C.V. et al., 2013. Partial diagenetic overprint of Late Jurassic belemnites
637   from New Zealand: Implications for the preservation potential of d7Li
638   values in calcite fossils. Geochimica Et Cosmochimica Acta, 120: 80–96.
639   van Geldern, R. et al., 2006. Carbon, oxygen and strontium isotope records of
640   Devonian brachiopod shell calcite. Palaeogeography Palaeoclimatology
641   Palaeoecology, 240: 47–67.
642   Vigier, N. et al., 2008. Quantifying Li isotope fractionation during smectite
643   formation and implications for the Li cycle. Geochimica Et Cosmochimica
644   Acta, 72: 780–792.
645   Vigier, N., Gislason, S.R., Burton, K.W., Millot, R., Mokadem, F., 2009. The
646   relationship between riverine lithium isotope composition and silicate
647   weathering rates in Iceland. Earth and Planetary Science Letters, 287(3-
648   4): 434–441.
649   Vigier, N., Rollion-Bard, C., Levenson, Y., Erez, J., 2015. Lithium isotopes in
650   foraminifera shells as a novel proxy for the ocean dissolved inorganic
651   carbon (DIC). Comptes Rendus Geoscience, 347: 43–51.
652   Walker, J.C.G., Hays, P.B., Kasting, J.F., 1981. A Negative Feedback Mechanism for
653   the Long-Term Stabilization of Earths Surface-Temperature. Journal of
654   Geophysical Research-Oceans and Atmospheres, 86(NC10): 9776-9782.
655   Whittle, G.L., Kendall, C.G.S.C., Dill, R.F., Rouch, L., 1993. Carbonate cement fabrics
656   displayed: A traverse across the margin of the Bahamas Platform near Lee
657   Stocking Island in the Exuma Cays. Marine Geology, 110: 213–243.
658   Wimpenny, J. et al., 2015. Lithium isotope fractionation during uptake by
659   gibbsite. Geochimica Et Cosmochimica Acta, 168: 133–150.

660   Wimpenny, J. et al., 2010. The behaviour of Li and Mg isotopes during primary
661   phase dissolution and secondary mineral formation in basalt. Geochimica
662   Et Cosmochimica Acta, 74: 5259-5279.
663   Wright, V.P., Burgess, P.M., 2005. The carbonate factory continuum, facies
664   mosaics and microfacies: an appraisal of some of the key concepts
665   underpinning carbonate sedimentology. Facies, 51: 17–23.
666   You, C.F., Chan, L.H., Gieskes, J.M., Klinkhammer, G.P., 2003. Seawater intrusion
667   through the oceanic crust and carbonate sediment in the Equatorial
668   Pacific: Lithium abundance and isotopic evidence. Geophysical Research
669   Letters, 30.
670   Zhang, S. et al., 2017. Investigating controls on boron isotope ratios in shallow
671   marine carbonates. Earth and Planetary Science Letters, 458: 380–393.
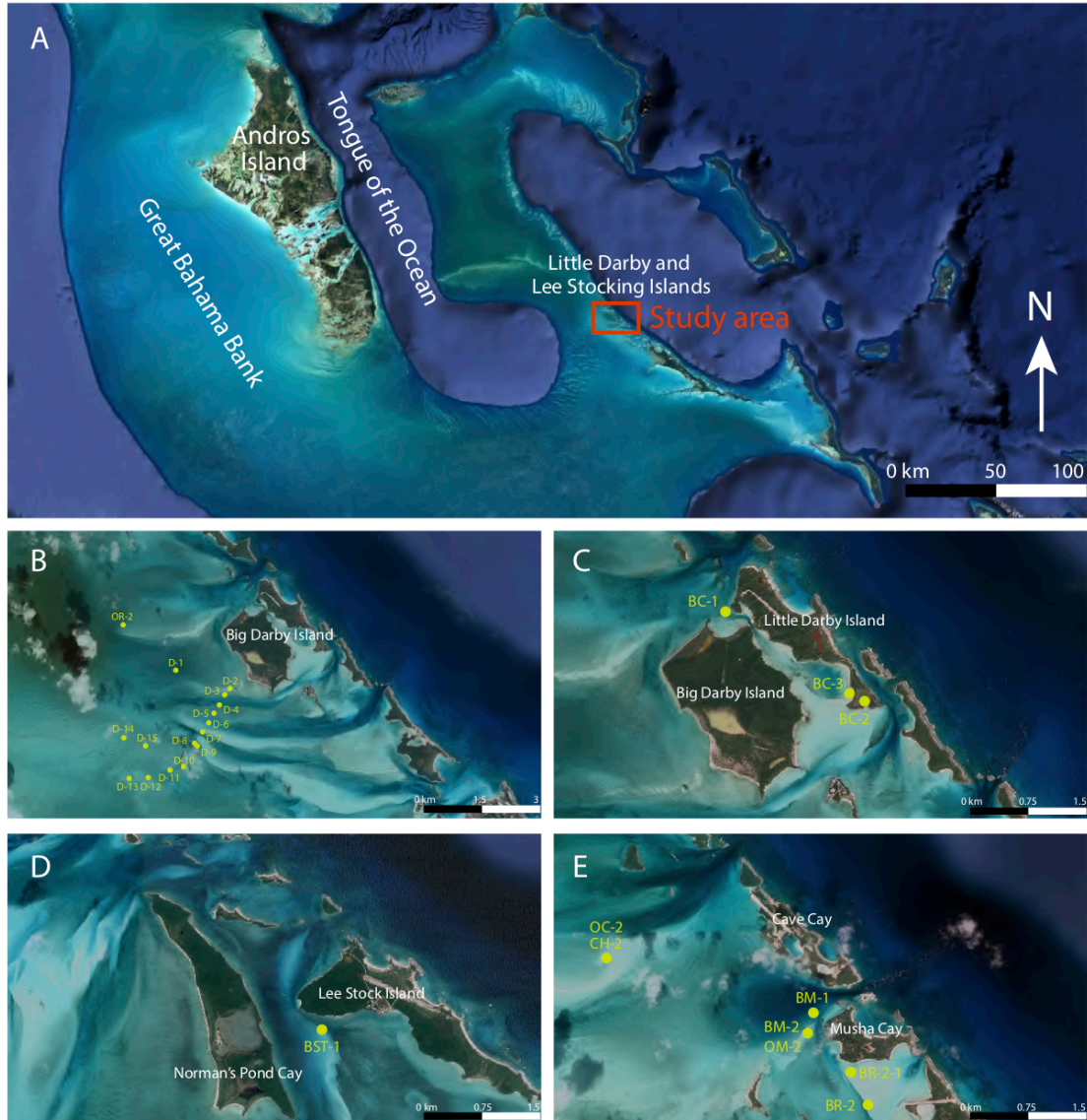672

673

674

675
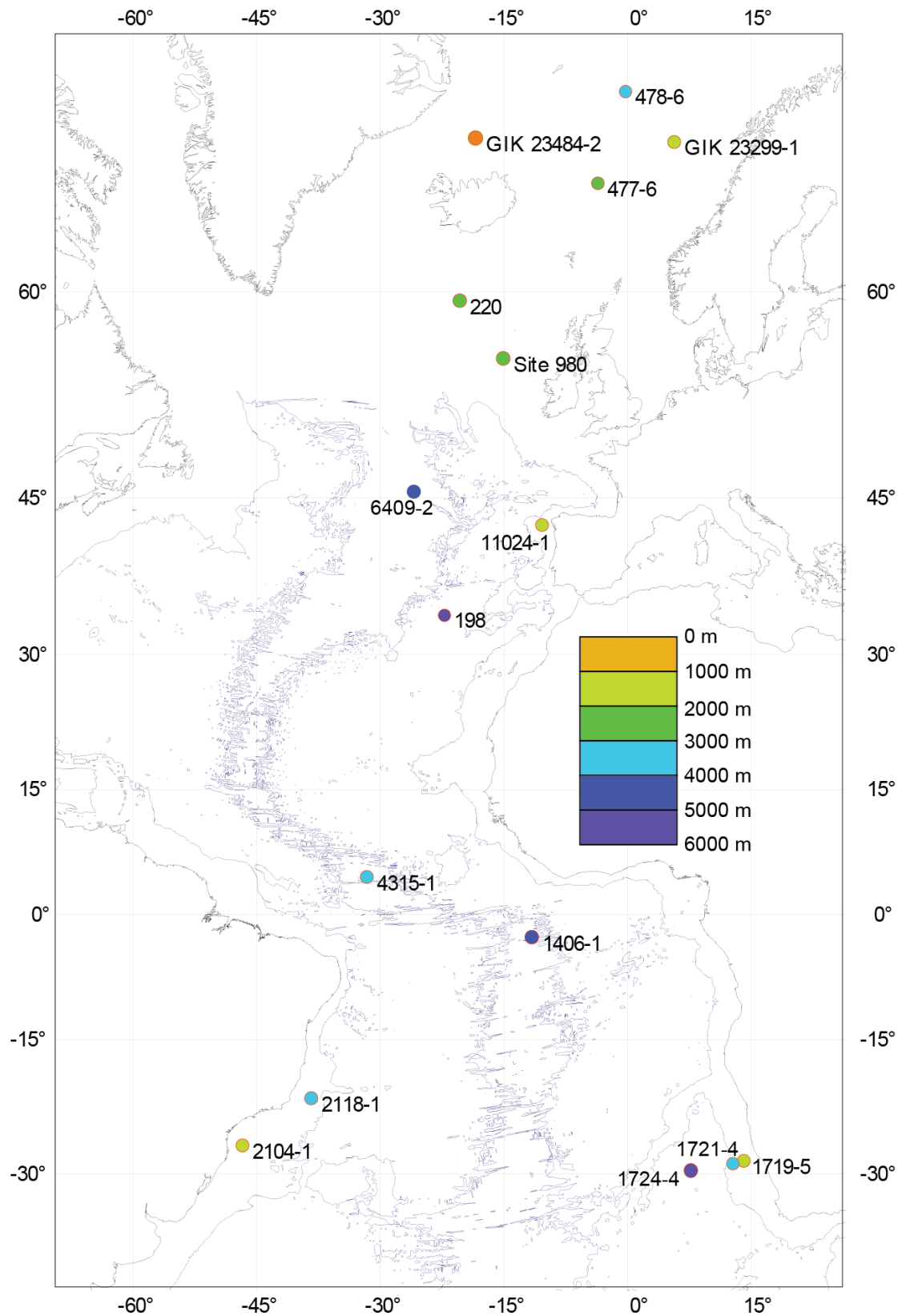
676 Figure 1. Sample location map for the core tops. The 4000m contour is also shown.

677 Symbol colours represent the broad depth scale.

678

679

680 Figure 2. Location of the examined surface samples from the Great Bahamas Bank.

681 All samples are from the Exuma Cays on the eastern edge of the Great Bahamas Bank

682 (A). Samples are from active ooid shoals (white regions) and from regions covered by

683 sparse to dense green algae and seagrass (darker regions). Samples are dominated by

684 sand size grains except for the sites with seagrass cover shown in panel B.

685
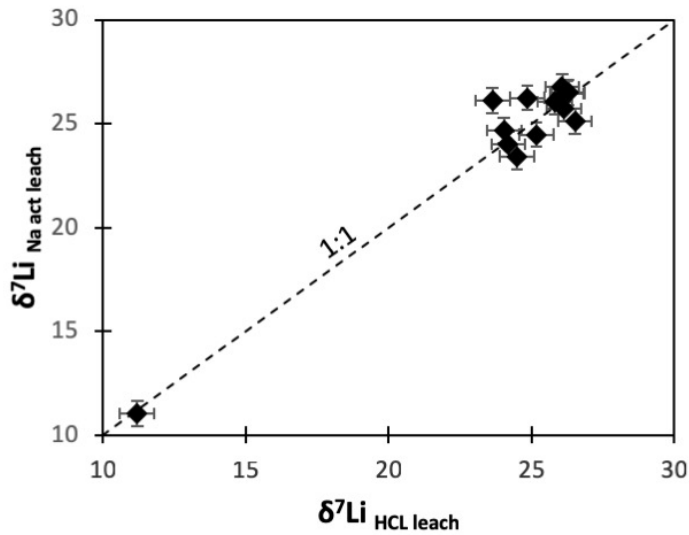
686

687

688 Figure 3. Comparison of δ^7Li from carbonate fractions leached by dilute HCl,

689 compared to those leached by acetic acid buffered with Na acetate. The dotted line

690 represents a 1:1 gradient. See text for details.

691
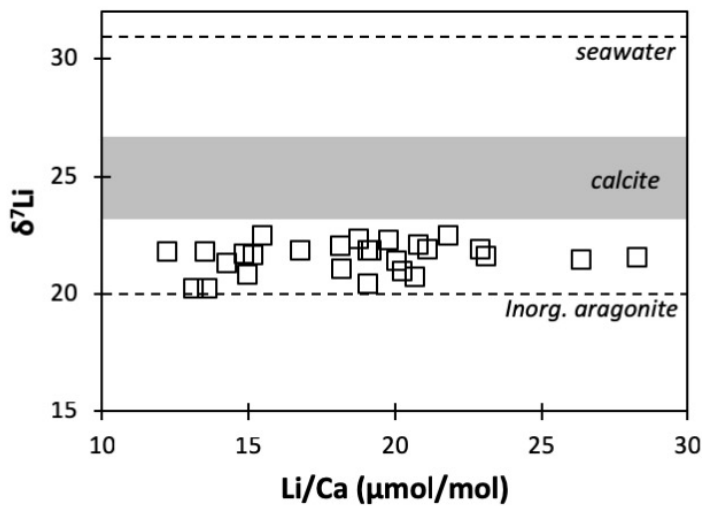
692

693 Figure 4. Li isotope ratios and Li/Ca ratios for the Bahamian samples. Analytical

694 uncertainty is smaller than the symbols. The grey box represents this study's core-top

695 samples. Values for inorganic aragonite and calcite precipitated from seawater are

696 from Marriott et al., 2004.

697

698

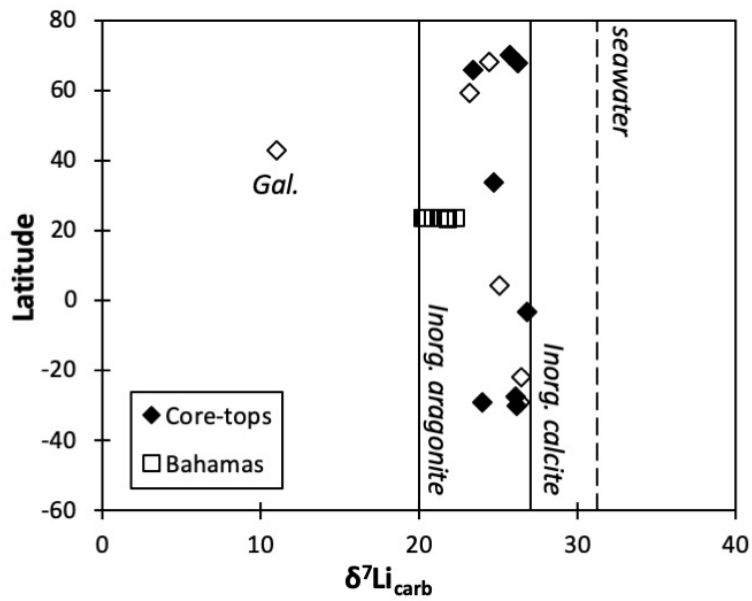699 Figure 5. Carbonate δ^7Li values for core-tops and the Bahamas plotted against sample

700 latitude. Open diamonds are samples with traces of aragonite. For the core-tops

701 (diamonds), the Na acetate leach values are shown. Values for inorganic aragonite and

702 calcite precipitated from seawater are from Marriott et al., 2004.

703
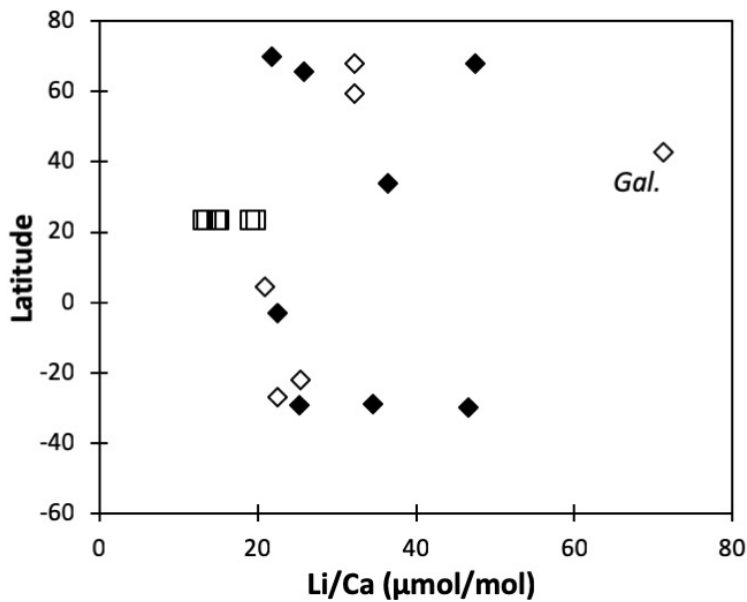
704

705 Figure 6. Carbonate Li/Ca ratios for the core-tops and the Bahamas plotted against

706 sample latitude. Open diamonds are samples with traces of aragonite. The Galician

707 coast sample GeoB 11024-1 is also highlighted.

708
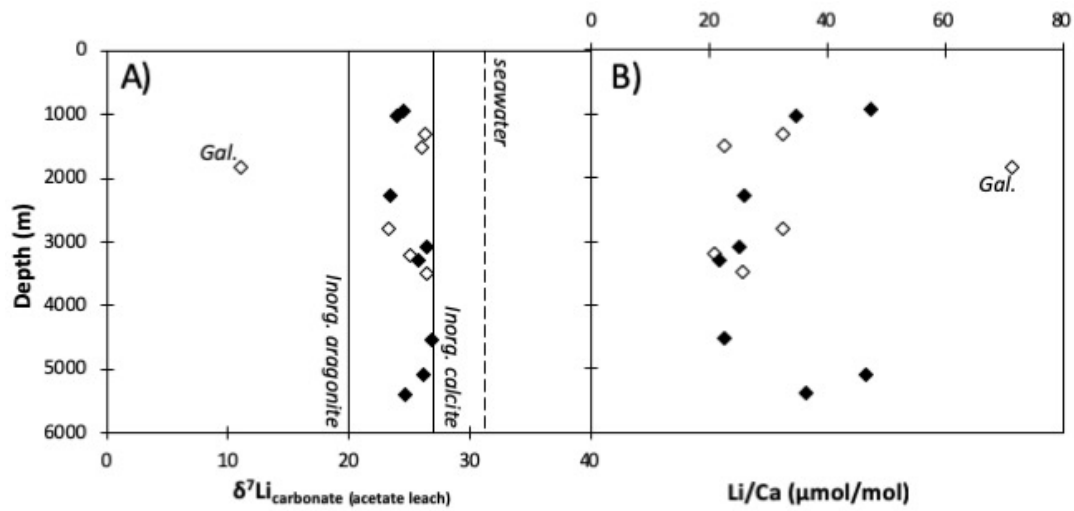
709

710   Figure 7. A) Core-top carbonate δ^7Li plotted against sample depth below sea-level.

711   Open symbols are samples with traces of aragonite. The sample from the Galician

712   coast GeoB 11024-1 is also highlighted. Values for inorganic aragonite and calcite

713   precipitated from seawater are from Marriott et al., 2004. B) Li/Ca values from the

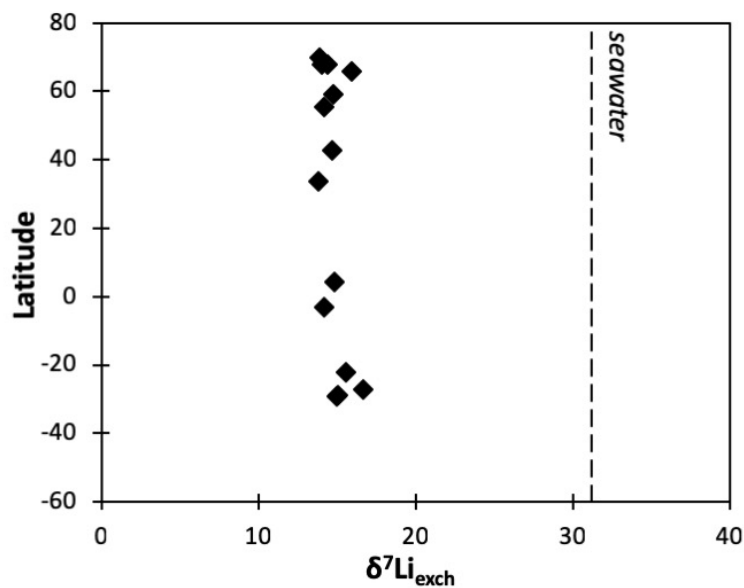714   same samples.

715

716

717   Figure 8. Core-top exchangeable Li isotope ratios plotted again sample latitude.

718

Cruise	Carbonate (HCl)										
	δ⁷Li	2sd	Li µg/g	Li/Ca µmol/mol	Mg/Ca mmol/mol	Al/Ca mmol/mol	Mn/Ca mmol/mol	Sr/Ca mmol/mol	δ⁷Li	2sd	Li/Ca µmol/m
M16-1	26.1	0.6	1.4	52.5	47.7	0.3	0.3	1.9	26.8	0.7	40.3
									25.9	0.2	43.1
M20-2	24.2	0.2	0.6	44.6	42.0	0.4	0.2	1.9	24.0	0.1	38.4
M20-2	26.2	0.2	0.6	35.2	36.8	0.1	0.5	1.1	26.4	0.3	35.4
M20-2	23.6	0.3	6.8	46.6	19.5	0.6	0.3	0.4	26.1	0.3	39.4
M23-2	25.8	0.2	1.3	22.5	14.6	0.1	0.2	0.8	26.1	0.2	20.4
									26.3	0.2	22.7
M23-2	26.3	0.3	1.2	35.5	31.3	0.3	0.2	1.4	26.5	0.1	36.1
											35.3
M38-1	26.5	0.6	1.0	30.9	43.3	0.2	0.3	1.7	25.1	0.5	28.8
M46-4											
Pos366-3	11.2	0.4	1.0	71.4	44.3	0.2	0.5	2.4	11.1	0.5	64.6
									11.7	0.5	60.2
M21-3	24.0	0.2	1.3	56.5	31.5	0.1	0.4	2.2	24.7	0.3	55.7
									25.5	0.1	56.2
M21-3	25.3	0.7	0.7	32.3	50.1	0.4	0.2	2.1	23.4	0.2	30.5
M26-2	24.5	0.5	0.8	45.9	17.3	0.3	0.2	2.1	23.4	0.8	45.1
M26-2	26.1	0.3	1.5	31.8	12.0	0.4	0.2	1.3	25.7	0.2	31.2
M7-3	24.8	0.4	1.1	32.3	12.4	0.4	0.3	1.4	26.2	0.4	31.9
M21-5	25.2	0.1	3.7	57.5	10.9	0.5	0.4	0.8	24.5	0.2	55.1
									24.1	0.2	53.1
ODP 162											
ples											
B-Massha 2	20.9	0.1		15.0	18.5	0.5		10.6			

719

720

Sample No.	Cruise	Lat	Long	Depth (m)	Remark	Residue		
						δ⁷Li	2sd	
1406-1	M16-1	-3.16	-11.23	4523		-1.8	0.1	2
rpt								
1719-5	M20-2	-28.93	14.17	1024		1.9	0.5	
1721-4	M20-2	-29.18	13.09	3079		1.2	0.1	
1724-4	M20-2	-29.98	8.04	5086		1.7	0.1	4
2104-1	M23-2	-27.29	-46.38	1505		-0.3	0.2	4
rpt								
2118-1	M23-2	-22.09	-38.02	3482		-0.4	0.2	1
rpt								
4315-1	M38-1	4.17	-31.28	3198		1.4	0.2	
rpt								
6409-2	M46-4	-44.51	-21.72	4296	(clay)	0.2	0.5	2
11024-1	Pos366-3	42.70	9.76	1831	(<63µm)	-1.5	0.2	4
rpt								
198	M21-3	33.81	-21.92	5389		1.9	0.1	2
rpt								
220	M21-3	59.26	-19.98	2797		1.2	0.4	
477-6	M26-2	65.82	-3.27	2275		2.6	0.4	
478-6	M26-2	70.00	0.06	3298		1.7	0.2	1
GIK 23299-1	M7-3	67.78	6.01	1305		1.2	0.2	2
GIK 23484-2	M21-5	67.94	-18.04	930		1.7	0.4	3
rpt								
Site 980	ODP 162	55.48	-14.70	2179	(decarbonated)	0.3	0.3	7
Bahamas samples					**Site description**			**Sampl**
BM-2	B-Massha 2	23.541	-76.168		unvegetated shoals			superfi
BR-2-1	B-Rudder 2	23.535	-76.154		unvegetated shoals			superfi
OM-2	Ooid Massha 2	23.537	-76.161		unvegetated shoals			superfi
BC-2	B-core 2	23.505	-76.124		sparse green algae and seagrass			peloids

721

722

723

| Cruise | CaCO$_3$ | TOC | Aragonite | Grain size | | CaCO$_3$ | TOC | CaCO$_3$ | CaCO$_3$ | Fine fraction by weight |
| | | | | % | % | | | % | % <20μm | |
	% bulk	%	wt.-%	<20μm	>20μm	% >20μm		>20μm	calc.	%
M16-1	65.0	0.9		25.0	75.0	73.6	0.71	55.2	9.8	66.4
M20-2	76.4	2.4		24.7	75.3	93.2	0.32	70.2	6.2	67.3
M20-2	84.8	0.4								64.9
M20-2	4.2	0.5								41.5
M23-2	18.4	1.2								80.3
M23-2	66.8	0.2		32.6	67.4	76.5	0.17	51.5	15.3	40.6
M38-1	81.4		16.7	45.9	54.1	60.3	0.59	32.6	48.8	46.7
M46-4										
Pos366-3										65.0
M21-3	58.0	0.6		92.0	8.0	60.0	0.48	4.8	53.2	94.3
M21-3	69.2	0.3		36.7	63.3	79.6	0.25	50.4	18.8	41.1
M26-2	80.2	0.5		25.0	75.0	70.0	0.33	52.5	27.7	36.9
M26-2	48.3	1.1		78.6	21.4	44.3	1.10	9.5	38.9	89.9
M7-3	41.0	0.9		86.1	13.9	39.0	0.96	5.4	35.5	97.2
M21-5										72.1

Table 3. Carbonate mineralogy and observational contents of the core-top samples.

724